Data in brief 23 (2019) 103719

Contents lists available at ScienceDirect

Data in brief

journal homepage: www.elsevier.com/locate/dib

Data Article

Spectroscopic and morphological data assessing the apatite forming ability of calcium hydroxide-releasing materials for pulp capping

Michele Di Foggia [a], Carlo Prati [b], Maria Giovanna Gandolfi [c], Paola Taddei [a, *]

[a] Biochemistry Unit, Department of Biomedical and Neuromotor Sciences, University of Bologna, Via Belmeloro 8/2, 40126 Bologna, Italy
[b] Endodontic Clinical Section, Unit of Odontostomatological Sciences, Department of Biomedical and Neuromotor Sciences, University of Bologna, Via San Vitale 59, 40136 Bologna, Italy
[c] Laboratory of Biomaterials and Oral Pathology, Unit of Dental Sciences, Department of Biomedical and Neuromotor Sciences, University of Bologna, Via San Vitale 59, 40136 Bologna, Italy

ARTICLE INFO

Article history:
Received 11 January 2019
Received in revised form 20 January 2019
Accepted 24 January 2019
Available online 7 March 2019

ABSTRACT

A pulp capping material must perform as a barrier and protect the dental pulpal complex by inducing the formation of a new dentin bridge or dentin-like tissue.
Being a favorable condition for the healing process, the apatite forming ability of TheraCal (light-curable Portland-dimethacrylate cement) and Dycal (calcium hydroxide-based) pulp capping materials was studied in two simulated body fluids, i.e. Dulbecco's Phosphate Buffered Saline (DPBS) and Hank's Balanced Salt Solution (HBSS). The cements were analyzed before and after soaking in these media for different times (1–28 days) by ESEM-EDX, micro-Raman and IR spectroscopy. This data article refers to "An in vitro study on dentin demineralization and remineralization: collagen rearrangements and influence on the enucleated phase" (Di Foggia et al., 2019).

* Corresponding author.
E-mail address: paola.taddei@unibo.it (P. Taddei).

https://doi.org/10.1016/j.dib.2019.103719

Specifications table

Subject area	Chemistry
More specific subject area	Materials chemistry
Type of data	Table, images, graphs, figures
How data was acquired	Micro-Raman spectroscopy (Jasco NRS-2000C); Fourier Transform FT-IR spectroscopy (Nicolet 5700, Thermo Electron Scientific Instruments Corp.) in ATR mode (Smart Orbit, diamond crystal); environmental scanning electron microscopy (ESEM Zeiss EVO 50, Carl Zeiss) with energy dispersive X-ray analysis EDX (Oxford INCA 350 EDS).
Data format	Raw and analyzed.
Experimental factors	TheraCal and Dycal commercial cements for pulp capping, prepared according to manufacturers' directions.
Experimental features	Micro-Raman, IR and ESEM-EDX analyses of the cements before and after soaking for 1−28 days in simulated body fluids, i.e. Dulbecco's Phosphate Buffered Saline (DPBS) or Hank's Balanced Salt Solution (HBSS).
Data source location	Bologna, Italy, University of Bologna (44.49381, 11.33875).
Data accessibility	The data is available with this article.
Related research article	M. Di Foggia, C. Prati, M. G. Gandolfi, P. Taddei, An in vitro study on dentin demineralization and remineralization: collagen rearrangements and influence on the enucleated phase, Journal of Inorganic Biochemistry, doi.org/10.1016/j.jinorgbio.2019.01.004. [1].

Value of the data

- Vibrational spectroscopy proved suitable to characterize the different phases present in the cement formulations.
- Spectroscopic techniques can provide useful information on material surface architecture of pulp capping materials as well as its evolution with ageing.
- Raman and IR spectra allow for evaluation of the relative thickness and maturation of the calcium phosphate phase formed upon soaking in simulated body fluids.

1. Data

The Raman and IR spectra of the fresh TheraCal cement (i.e. upon light-curing, Fig. 1) were in agreement with its formulation (Table 1); ESEM-EDX analysis showed a granular surface displaying many element peaks (Ca, Si, W, Ba, Al, S) (Fig. 2). The comparison with the IR spectrum of the resin (Fig. 3) allowed to assign the bands due to the organic phase (methacrylate-based resin; bisphenol A-based component [2], photoinitiator) and inorganic components (barium sulphate, alite, belite, tricalcium aluminate [3,4], silica [5] and calcium tungstate [6].

The spectra of fresh Dycal (i.e. upon setting, Fig. 4) showed the presence of a salicylate ester, calcium hydroxide, zinc oxide, calcium tungstate, titanium oxide as anatase, and calcium phosphate. If compared with the IR spectra of the catalyst and base pastes (Fig. 5), the IR spectrum of the cement (i.e. upon setting) shows the disappearance of the phenolic OH stretching band at 3170 cm^{-1}, the shift of the C═O stretching mode from 1725 to 1669 cm^{-1} to 1660 cm^{-1}, and the appearance of the COO^- stretching mode at 1538 cm^{-1}, according to the cement hardening mechanism proposed in the literature [6]. Freshly prepared Dycal samples (Fig. 6) showed a flat homogeneous surface and displayed Ca, S, P, Zn, Ti and W peaks.

Fig. 1a and b shows the IR and Raman spectra recorded on TheraCal after ageing in DPBS. After one day of ageing, a thick deposit of nanospherulites (showing Ca and P peaks at EDX, Fig. 2) formed, and the bands due to the underlying cement became undetectable in both IR and micro-Raman spectra. The position and broadening of the 952 cm^{-1} Raman band and the lack of resolution of the 549 cm^{-1} IR component suggested that calcium phosphate deposits on TheraCal were poorly crystalline. However, from 7 days onwards, the deposits attained a higher degree of crystallinity (Raman band at 959 cm^{-1} and IR bands at 600-560 cm^{-1}) and the bands typical of a B-type carbonated apatite [7] were observed.

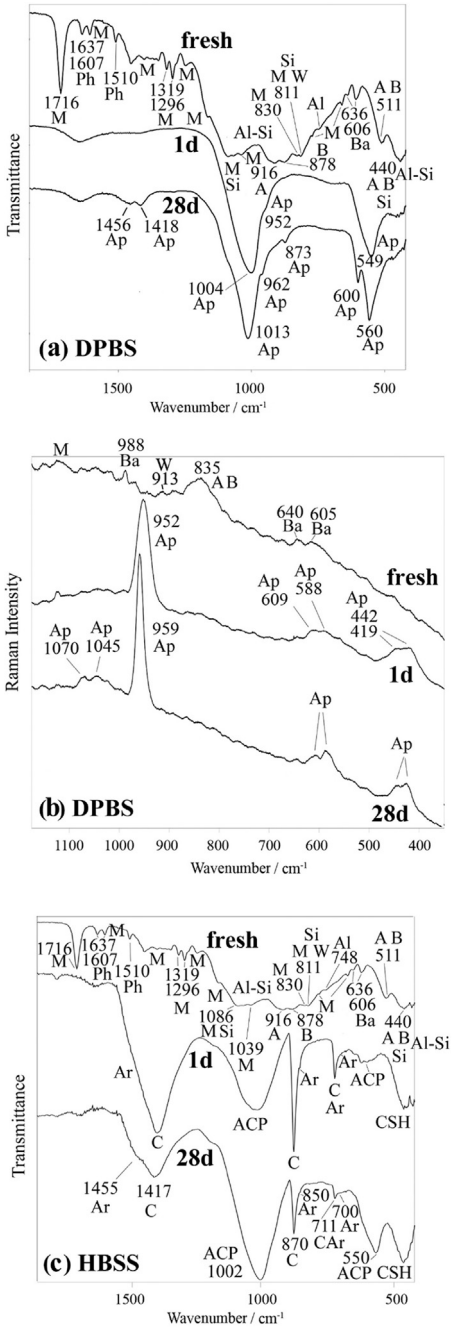

Fig. 1. (a) Average IR and (b) micro-Raman spectra of TheraCal before (i.e. fresh) and after immersion in DPBS; (c) average IR spectra of TheraCal before and after immersion in HBSS. The bands prevalently due to alite (A), belite (B), tricalcium aluminate (Al), methacrylate-based resin (M), aromatic component (Ph), barium sulphate (Ba), aluminosilicate glass (Al-Si), silica (Si), calcium tungstate (W), apatite (Ap), calcite (C), aragonite (Ar), silicate hydrate gel (CSH) and amorphous calcium phosphate (ACP) are indicated.

Table 1
Detailed composition of TheraCal and Dycal cements.

Material	Manufacturer and lot number	Composition
Dycal	Dentsply, USA, lot. 081007	**Base paste:** 1,3-butylene glycol disalicylate, zinc oxide, calcium phosphate, calcium tungstate, iron oxide pigments. **Catalyst paste:** calcium hydroxide, N-ethyl-o/p-toluene sulphonamide, zinc oxide, titanium oxide, zinc stearate, iron oxide pigments.
TheraCal	Bisco Inc., USA,lot. 603-189-A	45% wt mineral material (type III Portland cement), 10% wt radiopaque component, 5% wt hydrophilic thickening agent (fumed silica) and approximately 45% resin. **Resin:** hydrophobic monomers such as urethane dimethacrylate (UDMA), bisphenol A-glycidyl methacrylate (BisGMA), triethylene glycol dimethacrylate (TEGDMA) and hydrophilic monomers such as hydroxyethyl methacrylate (HEMA) and polyethylene glycol dimethacrylate (PEGDMA).

Fig. 1c shows the IR spectra recorded on TheraCal upon ageing in HBSS; after one day, the spectral features typical of ACP (amorphous calcium phosphate) [8], calcite and aragonite [4,9] phases were detected, superimposed to the band of the silicate hydrate gel (CSH) [4]. At this stage, calcite appeared the most abundant phase. At 28 days of ageing, the bands of ACP increased their relative intensity,

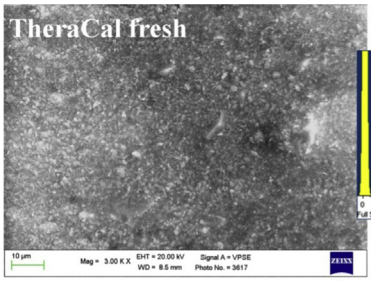

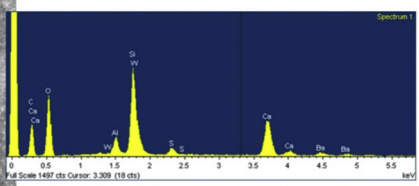

Element	Weight%	Atomic%
C K	28.37	40.62
O K	43.94	47.24
Al K	2.20	1.40
Si K	9.86	6.04
S K	1.08	0.58
Ca K	7.95	3.41
Ba L	2.81	0.35
W M	3.77	0.35
Totals	100.00	

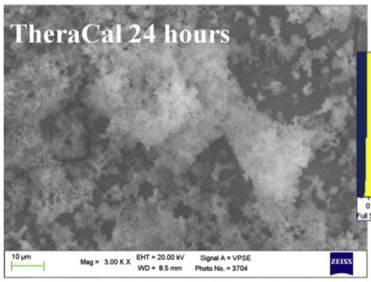

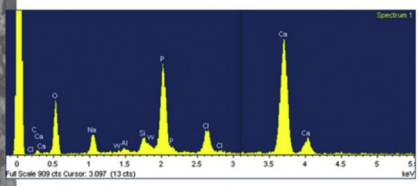

Element	Weight%	Atomic%
C K	7.18	11.65
O K	41.33	56.62
Na K	4.54	4.34
Si K	1.48	1.16
P K	13.78	9.77
Cl K	4.24	2.63
Ca K	26.87	14.72
W M	0.57	0.06
Totals	100.00	
Ca/P		1.51

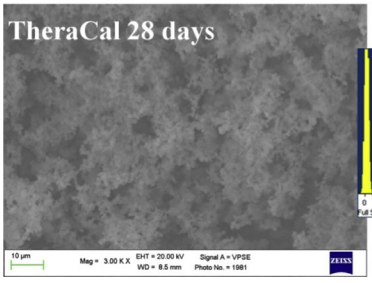

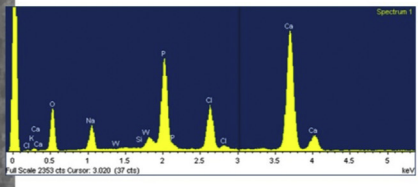

Element	Weight%	Atomic%
O K	41.30	61.07
Na K	5.90	6.07
P K	14.33	10.95
Cl K	8.03	5.36
K K	0.33	0.20
Ca K	27.03	15.96
W M	3.07	0.40
Totals	100.00	
Ca/P		1.46

Fig. 2. ESEM-EDX analyses of TheraCal samples before and after ageing in DPBS.

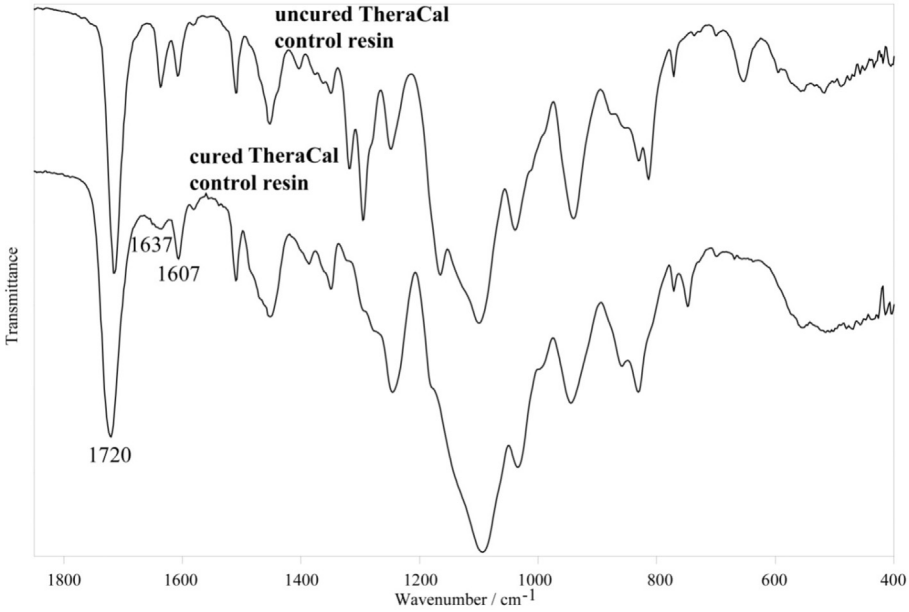

Fig. 3. Average IR spectra of uncured and cured TheraCal control resin.

together with an increase in Ca and P weight% (Fig. 2), suggesting a thickening of the deposit, which at this stage appeared prevalently formed by ACP; the band of the CSH phase below 500 cm^{-1} was still detected.

The spectra recorded on Dycal samples (Fig. 4a and b) at different ageing times in DPBS showed a progressive strengthening of the bands assignable to calcium phosphates (due to apatite deposition) and a weakening of those due to the material components (salicylate bands), which became undetectable in the IR spectra since 14 days. This trend suggests that calcium phosphate deposits (with granules measuring around 0.3–0.5 μm, Fig. 6) were formed on Dycal and covered the material components still present in the deeper cement composition. At micro-Raman analysis (Fig. 4b), the material components were still detectable after 28 days, suggesting the formation of a thin layer of apatite agglomerates (Fig. 6).

The IR spectra recorded on Dycal after 1 and 28 days of soaking in HBSS (Fig. 4c) showed with progressively increased intensity the bands due to the crystalline calcium phosphate component already present in the fresh cement, together with those of calcite and aragonite; the marker bands of the cement progressively weakened.

2. Experimental design, materials, and methods

2.1. Materials preparation and apatite forming ability tests

Dycal and TheraCal disks (8 mm diameter, 1.6 mm thick) were prepared according to the manufacturers' directions. Dycal was cured (37 °C, 98% relative humidity) for a period corresponding to 70% of the final setting time, i.e. 2 min. TheraCal samples were light-cured with a halogen lamp for 20 s on both surfaces.

To test the apatite forming ability of the materials, the disks were soaked in 10 mL of DPBS or HBSS at 37 °C, for 1–28 days. The soaking medium was renewed every week. The samples were analyzed before and after ageing by ESEM-EDX, micro-Raman and ATR-IR spectroscopic techniques.

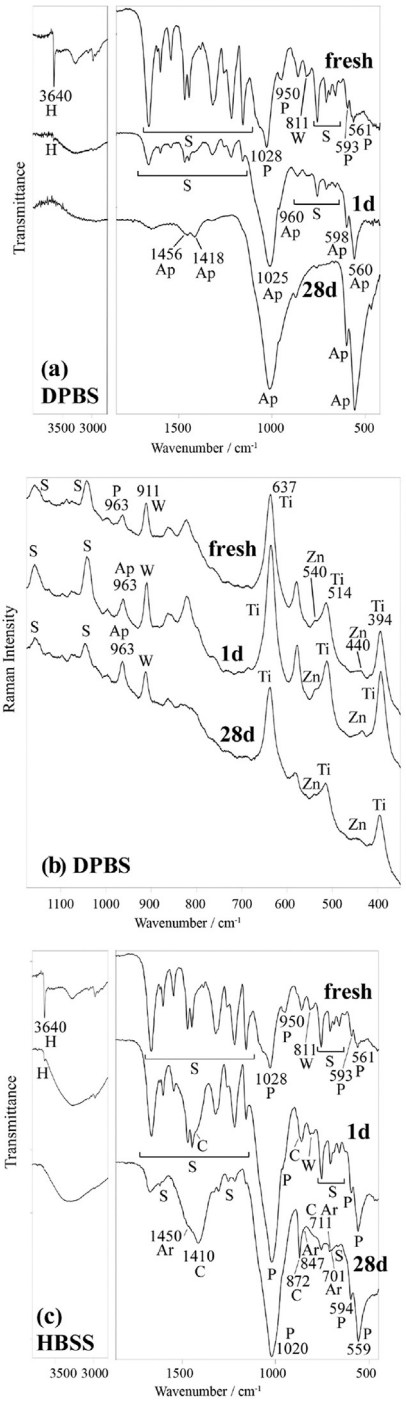

Fig. 4. (a) Average IR and (b) Raman spectra of Dycal before (i.e. fresh) and after immersion in DPBS; (c) average IR spectra of Dycal before and after immersion in HBSS. The bands prevalently due to salicylate ester (S), calcium tungstate (W), calcium phosphate (P), calcite (C), aragonite (Ar), titanium oxide as anatase (Ti), zinc oxide (Zn), apatite (Ap) and calcium hydroxide (H) are indicated.

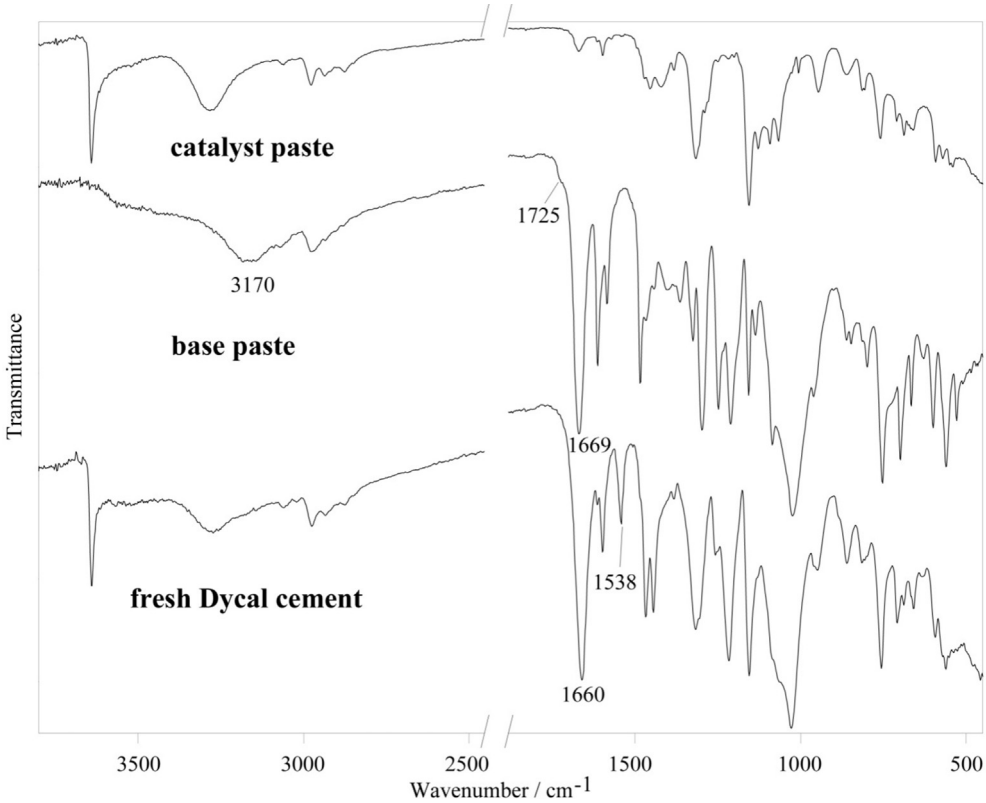

Fig. 5. Average IR spectra of fresh Dycal, catalyst and base pastes.

2.2. Vibrational spectroscopy

Micro-Raman spectra were obtained using a Jasco NRS-2000C instrument connected to a microscope with 20 × magnification. All the spectra were recorded in back-scattering conditions with 5 cm^{-1} spectral resolution (λ_{exc} = 514 nm, 50 mW) using a 160K-frozen charge coupled detector. IR spectra were recorded on a Thermo Electron Nicolet 5700 Fourier Transform FT-IR, equipped with a smart orbit diamond ATR accessory and a deuterated triglycine sulphate detector; the spectral resolution was 4 cm^{-1}. To minimize problems deriving from the possible sample inhomogeneity, at least five Raman and IR spectra were recorded on the upper surface of each specimen.

The degree of conversion (DC%, i.e. the percentage of double bond vinyl conversion, Fig. 7) of TheraCal formulation, TheraCal control paste and control resin was calculated from the IR spectra (Figs. 3, 8 and 9) [10] as:

$$DC\% = 100 \times \left[1 - \frac{\left(\frac{I_{C=C\ \text{aliphatic}}}{I_{C=O}} \right)_{\text{polymer}}}{\left(\frac{I_{C=C\ \text{aliphatic}}}{I_{C=O}} \right)_{\text{monomer}}} \right] \quad (1)$$

where $(I_{C=C\ \text{aliphatic}}/I_{C=O})_{\text{polymer}}$ and $(I_{C=C\ \text{aliphatic}}/I_{C=O})_{\text{monomer}}$ were the ratios between the intensities of the aliphatic C=C and C=O IR bands (at 1637 and 1716 cm^{-1}, respectively) calculated as peak heights from the IR spectra of the photopolymerized sample (i.e. TheraCal formulation or TheraCal control paste or control resin after light-curing) and unphotopolymerized sample (i.e. TheraCal formulation or TheraCal control paste or control resin before light-curing), respectively.

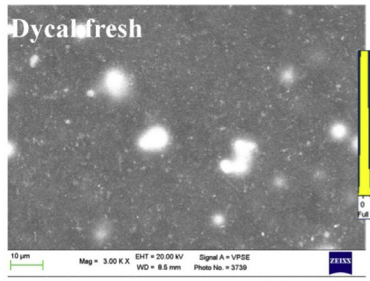

Element	Weight%	Atomic%
C K	30.43	46.76
O K	32.67	37.69
P K	2.29	1.36
S K	4.57	2.63
Ca K	17.52	8.06
Ti K	1.96	0.75
Zn K	9.26	2.61
W M	1.31	0.13
Totals	100.00	

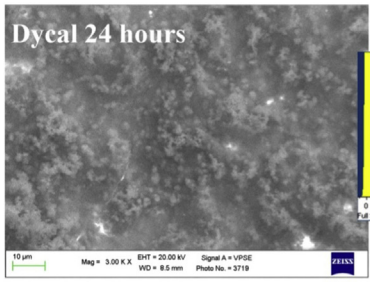

Element	Weight%	Atomic%
O K	42.25	61.46
Na K	6.54	6.62
P K	14.67	11.02
S K	1.24	0.90
Cl K	6.00	3.94
Ca K	24.83	14.42
Ti K	0.38	0.19
Zn K	4.08	1.45
Totals	100.00	
Ca/P		1.31

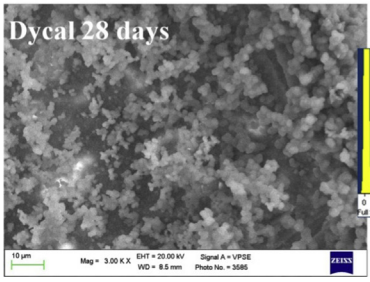

Element	Weight%	Atomic%
O K	42.97	62.98
Na K	3.76	3.84
P K	14.49	10.97
S K	0.39	0.29
Cl K	3.79	2.51
Ca K	31.00	18.14
Zn K	3.59	1.29
Totals	100.00	
Ca/P		1.65

Fig. 6. ESEM-EDX analyses of Dycal samples before and after ageing in DPBS.

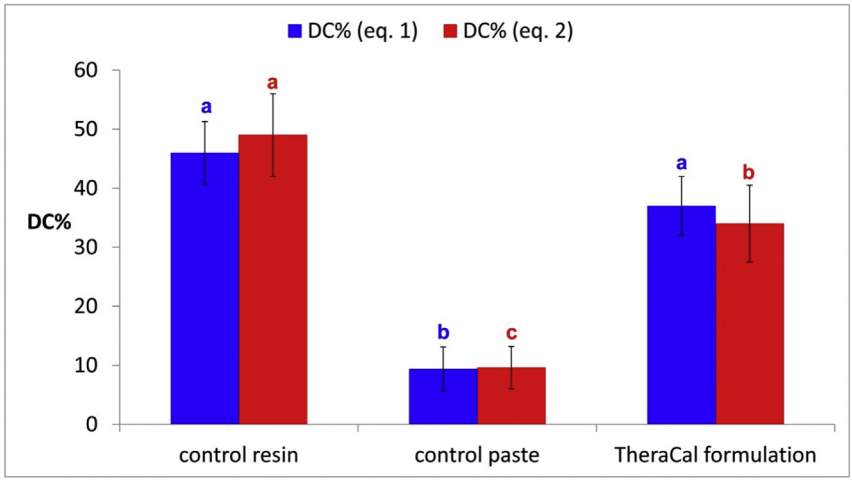

Fig. 7. DC% values (calculated according to Equations 1 and 2) for TheraCal formulation, control resin and control paste. Different letters on the histogram bars indicate significant differences among the data calculated by using each equation.

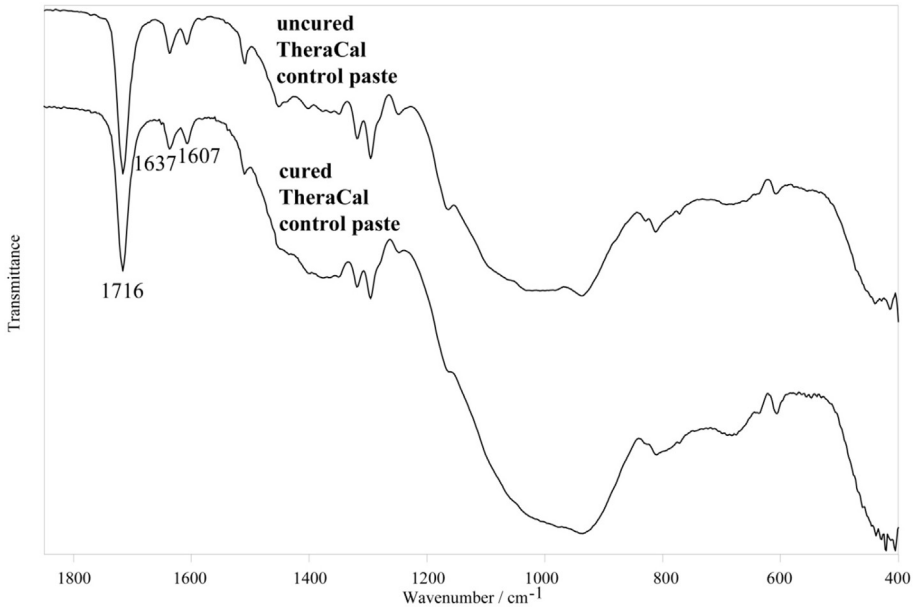

Fig. 8. Average IR spectra of uncured and cured TheraCal control paste (i.e. TheraCal formulation without bioactive oxides).

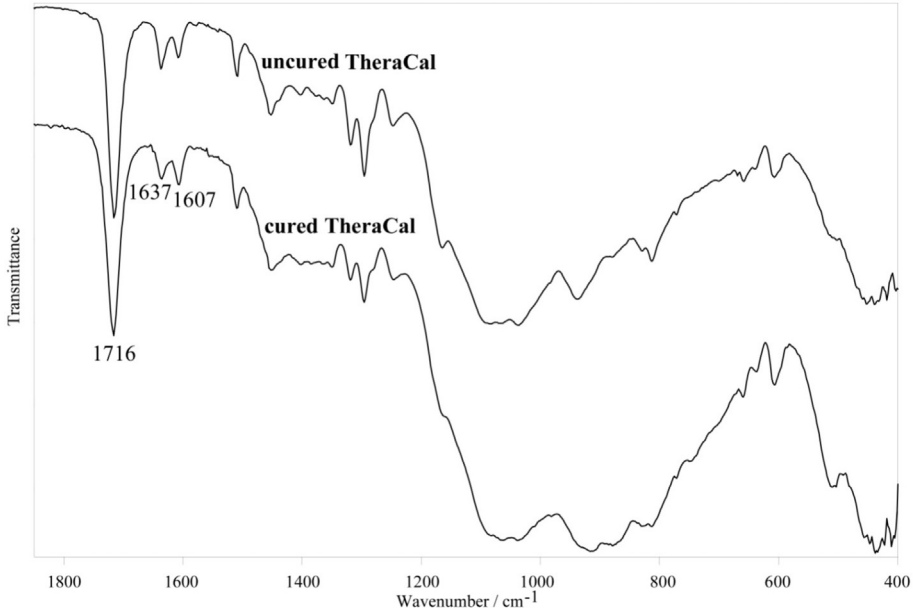

Fig. 9. Average IR spectra of uncured and cured TheraCal.

For confidential results, in agreement with previous studies on the photopolymerization of BisGMA-containing composites [2], the DC% was also calculated as:

$$DC\% = 100 \times \left[1 - \frac{\left(\frac{I_{C=C\ \text{aliphatic}}}{I_{C=C\ \text{aromatic}}}\right)_{\text{polymer}}}{\left(\frac{I_{C=C\ \text{aliphatic}}}{I_{C=C\ \text{aromatic}}}\right)_{\text{monomer}}}\right] \quad (2)$$

where $(I_{C=C\ \text{aliphatic}}/I_{C=C\ \text{aromatic}})_{\text{polymer}}$ and $(I_{C=C\ \text{aliphatic}}/I_{C=C\ \text{aromatic}})_{\text{monomer}}$ were the ratios between the intensities of the aliphatic and aromatic C=C IR bands (at 1637 and 1607 cm^{-1}, respectively) calculated as peak heights from the IR spectra of the photopolymerized sample (i.e. TheraCal formulation or TheraCal control paste or control resin after light-curing) and pre-photopolymerized sample (i.e. TheraCal formulation or TheraCal control paste or control resin before light-curing).

2.3. ESEM-EDX

Cement sample surfaces were examined with a Zeiss EVO 50 ESEM microscope with INCA 350 EDX at 20–25 kV accelerating voltage. Elemental analysis was performed applying the ZAF correction method. Wet specimens were placed directly on the ESEM stub and examined in wet conditions without any artifacts related to preparation/coating [11].

2.4. Statistical analysis

Data were analyzed applying the one-way ANOVA followed by Student-Newman-Keuls test using the Sisvar statistical software (Daniel Furtado Ferreira, Universidade Federal de Lavras/UFLA – Brasil). Statistical significance was set at $p < 0.05$.

Acknowledgments

This work was supported by RFO funds from University of Bologna.

Transparency document

Transparency document associated with this article can be found in the online version at https://doi.doi.org/10.1016/j.dib.2019.103719.

References

[1] M. Di Foggia, C. Prati, M.G. Gandolfi, P. Taddei, An in vitro study on dentin demineralization and remineralization: collagen rearrangements and influence on the enucleated phase, J. Inorg. Biochem. 193 (2019) 84–93, https://doi.org/10.1016/j.jinorgbio.2019.01.004.
[2] D. Manojlovic, M.D. Dramićanin, M. Milosevic, I. Zeković, I. Cvijović-Alagić, N. Mitrovic, V. Miletic, Effects of a low-shrinkage methacrylate monomer and monoacylphosphine oxide photoinitiator on curing efficiency and mechanical properties of experimental resin-based composites, Mater. Sci. Eng. C 58 (2016) 487–494.
[3] P. Taddei, A. Tinti, M.G. Gandolfi, P.L. Rossi, C. Prati, Ageing of calcium silicate cements for endodontic use in simulated body fluids: a micro-Raman study, J. Raman Spectrosc. 40 (2009) 1858–1866.
[4] P. Taddei, E. Modena, A. Tinti, F. Siboni, C. Prati, M.G. Gandolfi, Vibrational investigation of calcium silicate cements for endodontics in simulated body fluids, J. Mol. Struct. 993 (2011) 367–375.
[5] R.A. Nyquist, C.L. Putzig, M.A. Leugers, The Handbook of Infrared and Raman Spectra of Inorganic Compounds and Organic Salts, Academic Press, San Diego CA, 1997.
[6] H.J. Prosser, D.M. Groffman, A.D. Wilson, The effect of composition on the erosion properties of calcium hydroxide cements, J. Dent. Res. 61 (1982) 1431–1435.
[7] D.G.A. Nelson, J.D.B. Featherstone, Preparation, analysis, and characterization of carbonated apatites, Calcif. Tissue Int. 34 (1982) S69–S81.
[8] G. Xu, I.A. Aksay, J.T. Grooves, Continuous crystalline carbonate apatite thin films. A biomimetic approach, J. Am. Chem. Soc. 123 (2001) 2196–2203.
[9] F.Z. Zakaria, J. Mihaly, I. Sajò, R. Katona, L. Haiba, F.A. Aziz, J. Mink, FT-Raman and FTIR spectroscopic characterization of biogenic carbonates from Philippine venus seashell and Porites sp. coral, J. Raman Spectrosc. 39 (2008) 1204–1209.

[10] P. Taddei, C. Prati, M.G. Gandolfi, A poly(2-hydroxyethyl methacrylate)-based resin improves the dentin remineralizing ability of calcium silicates, Mater. Sci. Eng. C 77 (2017) 755–764.
[11] M.G. Gandolfi, P. Taddei, E. Modena, F. Siboni, C. Prati, Biointeractivity-related versus chemi/physisorption-related apatite precursor-forming ability of current root end filling materials, J. Biomed. Mater. Res. B Appl. Biomater. 101 (2013) 1107–1123.